

Broad Balmer-line Absorption in SDSS J172341.10+555340.5 *

Kentaro AOKI

*Subaru Telescope, National Astronomical Observatory of Japan, 650 North A'ohoku Place, Hilo,
HI 96720, U.S.A.*

(Received 2010 March 22; accepted 2010 July 26)

Abstract

I present the discovery of Balmer-line absorption from H α to H9 in iron low-ionization broad absorption line (FeLoBAL) quasar, SDSS J172341.10+555340.5 by near-infrared spectroscopy with the Cooled Infrared Spectrograph and Camera for OHS (CISCO) attached to the Subaru telescope. The redshift of the Balmer-line absorption troughs is 2.0530 ± 0.0003 , and it is blueshifted by 5370 km s^{-1} from the Balmer emission lines. It is more than 4000 km s^{-1} blueshifted from the previously known UV absorption lines. I detect relatively strong ($\text{EW}_{\text{rest}} = 20 \text{ \AA}$) [O III] emission lines which are similar to those found in other broad absorption line quasars with Balmer-line absorption. I derived a column density of neutral hydrogen of $5.2 \times 10^{17} \text{ cm}^{-2}$ by using the curve of growth and taking account of Ly α trapping. I searched for UV absorption lines which have the same redshift with Balmer-line absorption. I found Al III and Fe III absorption lines at $z=2.053$ which correspond to previously unidentified absorption lines, and the presence of other blended troughs that were difficult to identify.

Key words: galaxies: active—quasars: absorption lines—quasars: emission lines—quasars: individual (SDSS J172341.10+555340.5)

1. Introduction

Outflow phenomena are ubiquitous among active galactic nuclei (AGN) in several regimes of the full electromagnetic spectrum. Recent X-ray spectroscopic observations reveal blueshifted absorption lines from highly ionized species in many nearby Seyfert 1s (see reviews by Turner & Miller (2009)). Since their early discovery by Lynds (1967), broad absorption lines (BALs) in quasars have been well studied. The widths of BAL are typically $\sim 2000 - 20,000$

* Based on data collected at Subaru Telescope, which is operated by the National Astronomical Observatory of Japan.

km s⁻¹, and are blueshifted relative to emission lines from 2000 km s⁻¹ to as much as $\sim 0.2c$. Half of all quasars have intrinsic narrow absorption lines that have FWHMs of a few hundred km s⁻¹ and most often blueshifted from the emission-line redshift in quasars (Misawa et al. 2007; Ganguly & Brotherton 2008). Similar absorption lines are common in nearby Seyfert 1 galaxies. More than half of Seyfert 1s show C IV and N V absorption lines in their UV spectra (Crenshaw et al. 1999), and half of them show O VI absorption (Dunn et al. 2007). Crenshaw, & Kraemer (2005) point out that inner narrow-line region (NLR) clouds are the source of UV absorbers in the Seyfert galaxy NGC 4151 based on their similar kinematical characteristics and locations. Cecil et al. (2002) also suggests that the high-velocity clouds in NLR of Seyfert 2 galaxy NGC 1068 would resemble intrinsic narrow absorption lines if they were viewed against the nuclear continuum source.

It is important to understand outflows because they transfer nuclear gas from near the super massive black hole (SMBH) to the outer region of host galaxies. Thus, these outflows may be related to the co-evolution of the bulge and SMBH (Silk & Rees 1998; Fabian et al. 1999; Granato et al. 2004). We do not yet fully understand not only the theory of outflow phenomena but also the phenomenologies. Recent large surveys such as the Sloan Digital Sky Survey (SDSS; York et al. 2000) have discovered outflows from ions not previously detected (Hall et al. 2002). One recent example is Balmer-line BALs (Aoki et al. 2006; Hall 2007).

We discovered H α absorption in the broad H α emission line of the BAL quasar, SDSS J083942.11+380526.3 (hereafter SDSS J0839+3805) through near-infrared spectroscopy (Aoki et al. 2006). The presence of nonstellar H α absorption was known only in the Seyfert galaxy NGC 4151 at that time; thus, our discovery was the first case for quasars. SDSS J0839+3805 is a so-called many-narrow-trough FeLoBAL quasar (hereafter mntBAL) (Hall et al. 2002), which has tremendous number of UV absorption lines. Hall (2007) also discovered Balmer absorption lines in SDSS J125942.8+121312.6 (hereafter SDSS J1259+1213) from its SDSS spectrum. SDSS 1259+1213 is also a probably mntBAL. Motivated by these discoveries, I began a search for Balmer-line absorption in mntBALs. SDSS J172341.10+555340.5 (hereafter SDSS J1723+5553) is a mntBAL reported by Hall et al. (2002), and it is a bright quasar in the near-infrared ($J = 16.1$, and $K_s = 14.1$). I performed near-infrared spectroscopy of SDSS J1723+5553, and report in this paper my discovery of the Balmer line absorption in SDSS J1723+5553. I assume throughout this paper $H_0 = 70$ km s⁻¹ Mpc⁻¹, $\Omega_m = 0.3$, and $\Omega_\Lambda = 0.7$. Note that all wavelengths in this paper are vacuum wavelengths.

2. Observations and Data Reduction

The JH - and K -band spectra of SDSS J1723+5553 were obtained with the Cooled Infrared Spectrograph and Camera for OHS (CISCO; Motohara et al. 2002) attached to the Subaru 8.2 m telescope (Iye et al. 2004) on 2005 July 16 (UT), which was relatively clear night with good seeing (0. $''$ 5 in K band). I set the slit width to 0. $''$ 6, which results in a resolution of

56 and 60 Å in *JH*- and *K*-band (i.e., $R \sim 300 - 350$), respectively, which were measured by using night sky lines. The slit position angle was 0°. I obtained four and two exposures in *JH*- and *K*-band, respectively, dithering the telescope to observe the quasar at two positions with a separation of 10'' along the slit. The integration times on target were 1200 s (300 s \times 4) in *JH* band and 500 s (250 s \times 2) in *K* band. The A3 star SAO 030517 was observed immediately after exposures of SDSS J1723+5553 for sensitivity calibration and removal of atmospheric absorption lines.

The data were reduced using IRAF for the standard procedures of flat-fielding, sky subtraction, and residual sky subtraction. Wavelength calibration was performed using OH night-sky lines. The rms wavelength calibration error is 1.5 Å in *JH*- and 6.0 Å in *K*-band, corresponding to 36 km s⁻¹ at 16170 Å (redshifted position of the H β line of SDSS J1723+5553) and 80 km s⁻¹ at 21780 Å (redshifted H α line), respectively. The sensitivity calibration was performed as a function of wavelength, and the atmospheric absorption features were removed with the spectrum of SAO 030517.

3. Results

Figure 1 displays the *JH*-band spectrum of SDSS J1723+5553. The *JH*-band spectrum clearly shows several absorption lines near the H β emission line and [O III] emission lines. H γ emission line is also identified although it overlaps with the atmospheric absorption lines. The small bumps at 12760 Å and 12300 Å correspond to H δ and H ϵ emission lines, respectively. The absorption lines must be Balmer-line absorption since most of them occur at the edge of blue wing of the broad Balmer emission lines. I fit the *JH*-band spectrum with a combination of a linear continuum, four Balmer emission lines from H β to H ϵ , six Balmer absorption lines from H β to H9, and [O III] $\lambda\lambda$ 4960, 5008.2 emission lines. All Balmer emission and absorption lines are fitted with a single Gaussian except for the H β emission line, which is fitted with a combination of two Gaussians. I fit the [O III] doublet $\lambda\lambda$ 4960.3, 5008.2 with a single Gaussian for each line. The width and redshift are assumed to be the same for both of the two [O III] lines and an intensity ratio of [O III] λ 5008/ λ 4960 fixed to be 3.0. The FWHM is corrected for the instrumental broadening by using the simple assumption: $\text{FWHM}_{\text{true}} = (\text{FWHM}_{\text{obs}}^2 - \text{FWHM}_{\text{inst}}^2)^{1/2}$, where FWHM_{obs} is the observed FWHM of the line and FWHM_{inst} is the instrumental FWHM. The results of fitting are tabulated in table 1. The FWHM_{true} of H β emission line is 3780 ± 150 km s⁻¹. The redshifts of Balmer emission lines from H β to H ϵ vary from 2.097 to 2.111. However, the H β emission line has much better signal-to-ratio than other Balmer emission lines. Also, the redshift of the H α emission line described below is same as that of the H β emission line. Therefore, I adopt 2.1080 ± 0.0001 as the redshift of broad emission line.

The redshifts of the Balmer-line series absorption troughs range from 2.0527 (H β) to 2.0540 (H9). The redshift of the H8 (λ 3890.2 Å) absorption line is smaller than other Balmer lines due to probably contamination of HeI 3889.7. Since the H9 absorption line is much weaker

than the other Balmer absorption lines, I adopt 2.0530 ± 0.0003 as the redshift of the system. This blueshift translates to an outflow velocity of 5370 km s^{-1} and a FWHM_{obs} of $700 - 1500 \text{ km s}^{-1}$. Because the $\text{FWHM}_{\text{inst}}$ is 1160 km s^{-1} in the JH band, the lines are not fully resolved. Although the $\text{FWHM}_{\text{true}}$ of the absorption lines have large uncertainties, the FWHM of the Balmer lines are consistent with Fe III and Al III absorption lines at the same redshift (described in 4.2). I present the equivalent widths (EWs) of the Balmer absorption troughs in table 2. I do not include broad emission lines for the continuum levels when I calculate the EWs.

I detect the relatively strong ($\text{EW}_{\text{rest}} = 20.3 \pm 0.1 \text{\AA}$) [O III] emission lines, which is common among four Balmer-lines BAL AGN (NGC 4151, SDSS 0839+3805, SDSS J1259+1213 and SDSS J1723+5553). I find a redshift for the [O III] emission of 2.1095 ± 0.0004 . Thus, the [O III] emission line is redshifted by 145 km s^{-1} relative to the broad emission line. The width of the [O III] emission line is resolved and the $\text{FWHM}_{\text{true}}$ is $1550 \pm 70 \text{ km s}^{-1}$. The optical luminosity of SDSS 1723+5553, $\log \lambda L_{\lambda}(5100)$ is 47.02 erg s^{-1} after correction for reddening ($E(B-V) = 0.25 \text{ mag}$). Compared with similar luminous quasars (Netzer et al. 2004), this line width is normal.

The K -band spectrum is displayed in Fig. 2. The strong H α emission is associated with a weak absorption line. I fit the K -band spectrum with a linear continuum, H α broad emission line, and H α absorption line. The H α emission line is modeled with a combination of three Gaussians, and the H α absorption line is fitted with a single Gaussian. The results are tabulated in table 1 and 2. The redshift of the H α emission line agrees with that of the H β emission line. The $\text{FWHM}_{\text{true}}$ of H α is 2780 km s^{-1} and it is 40% smaller than the $\text{FWHM}_{\text{true}}$ of H β . This difference between the width of H α and H β is larger than the 17% found by Greene & Ho (2005) among 160 sample of AGN.

The redshift of the H α absorption line is smaller than that of the H β absorption line. However, the H α absorption line is overlapped with the strong atmospheric absorption line at $2.00 \mu\text{m}$ (figure 2). Thus, the redshift of the H α absorption line is less accurate than that of H β absorption line.

4. Discussion

4.1. Balmer absorption lines

The Balmer absorption lines found in SDSS J1723+5553 are from an outflow phenomenon from the nucleus, not from the host galaxy. First, the Balmer absorption lines are blueshifted by 5370 km s^{-1} from the emission lines. Second, there are Fe III and Al III absorption lines at the same redshift of the Balmer absorption lines (see §4.2). This is not the case in post-starburst galaxies which exhibit strong Balmer absorption lines.

In order to derive the column density of neutral hydrogen from the unresolved Balmer absorption lines, I use the curve of growth (Spitzer 1978). I fit for the Doppler parameter, b ,

and the column density of neutral hydrogen at the $n=2$ level (e.g., Savaglio et al. 2003). The resulting best-fit curve of growth is shown in figure 3. I derived $(1.5 \pm 0.9) \times 10^{15} \text{ cm}^{-2}$ for the hydrogen column density at $n=2$ level and $75 \pm 25 \text{ km s}^{-1}$ for b . As pointed out in §3, the H8 absorption line is probably contaminated by a He I absorption line. The strength of H8 clearly deviates from the curve of growth in figure 3. This also supports possible contamination of He I, and therefore I do not use H8 for the fitting. The Doppler parameter $b = 75 \text{ km s}^{-1}$ corresponds to a FWHM of 125 km s^{-1} . This FWHM is much smaller than those I measure in §3 ($700 - 1500 \text{ km s}^{-1}$). This fact suggests that the absorption lines consist of separated narrow (FWHM = $100 - 200 \text{ km s}^{-1}$), but not strongly saturated components. Such narrow separated components are in fact observed with high resolution spectroscopy in FeLoBALs, QSO 2359-1241 (Arav et al. 2008), SDSS J0318-0600 (Dunn et al. 2010) and AKARI-IRC 1757+5907 (Aoki et al, in preparation). In such cases, velocity width derived from low resolution spectroscopy indicates a relative distribution in velocity range of narrow components, not the width of each component. However, the equivalent width is not affected by the low resolution. The Doppler parameter derived from the curve of growth method should be much smaller than the velocity width measured by low resolution spectroscopy. Since I do not resolve the absorption lines, I can not estimate the covering factor. Thus, I assume the covering factor of the absorber of the continuum is 1. If the covering factor is significantly smaller than 1, as estimated for SDSS J1259+1213 by Hall (2007), the column density estimated above would be lower limit.

The optical depth at the center of the $H\beta$ absorption line ($\tau_{H\beta}$) is estimated to be 17 (Eq. (3-51) of Spitzer (1978)). Such a large $\tau_{H\beta}$ results in a large $\tau_{Ly\alpha}$ since $\tau_{H\beta}$ and $\tau_{Ly\alpha}$ follow the relationship,

$$\tau_{Ly\alpha} = \frac{\lambda_{Ly\alpha} f_{Ly\alpha}}{\lambda_{H\beta} f_{H\beta}} \frac{N_1}{N_2} \tau_{H\beta} = 0.87 \frac{N_1}{N_2} \tau_{H\beta}, \quad (1)$$

where λ is wavelength, f is oscillator strength, and N_1 and N_2 are the population of the level $n=1$ and $n=2$, respectively (Hall 2007). As pointed out by Hall (2007), when $\tau_{Ly\alpha}$ is large, every $Ly\alpha$ photon created by recombination is absorbed $\tau_{Ly\alpha}$ times before it escapes, and excites a hydrogen atom to its $n=2$ level. The $n=2$ level population for a given temperature is thus increased by a factor of $\tau_{Ly\alpha}$ from the thermal equilibrium,

$$\frac{N_1}{N_2} = \frac{1}{4} \exp(10.2 \text{ eV}/kT) \frac{1}{\tau_{Ly\alpha}} \quad (2)$$

(Hall 2007). Substituting our $\tau_{H\beta}$ and $T = 7500 \text{ K}$ (Osterbrock & Ferland 2006) into (1) and (2), I derive $\tau_{Ly\alpha} = 5140$, and $\frac{N_1}{N_2} = 348$. The neutral hydrogen column density is derived to be $5.2 \times 10^{17} \text{ cm}^{-2}$.

4.2. Metal absorption lines at $z=2.053$

The Balmer-line absorption of SDSS J1723+5553 I have discovered has a redshift of 2.053. It is $> 4000 \text{ km s}^{-1}$ blueshifted from the previously known absorption lines. Hall et

al. (2002) identified three absorption lines systems ($z = 2.0942, 2.100$, and 2.1082) in the rest UV spectrum. In order to check whether $z = 2.053$ UV metal absorption lines exist, I examine the UV spectrum of SDSS J1723+5553 from the SDSS Data Release 5. I have searched for the $z = 2.053$ absorption lines from the list by Hall et al. (2002) between 3800 \AA and 9000 \AA , which corresponds to a rest wavelength range of 1245 \AA and 2947 \AA . Many absorption lines from the $z = 2.0942, 2.100$ and 2.1082 systems exist in the UV spectrum. Because these troughs are blending, it is difficult to identify $z = 2.053$ absorption lines. At least Fe III UV34 $\lambda\lambda 1914.1, 1926.3$ and Al III $\lambda\lambda 1854.7, 1862.8$ at $z = 2.053$ are convincingly identified (figure 4) although other absorption at $z = 2.053$ probably exists and is hidden by severe overlap with absorption at $z = 2.0942, 2.100$ and 2.1082 . I describe in detail the identifications of those three absorption in following paragraphs.

The Al III $\lambda\lambda$ doublet $1854.7, 1862.8$ with a redshift of 2.053 corresponds to the trough between 5660 \AA and 5690 \AA in the observed frame. I compare the region between 1700 and 2000 \AA of SDSS 1723+5553 with those of other Balmer BAL AGN (NGC 4151 and SDSS J0839+3805)¹. The spectrum of NGC 4151 was taken in 1999 July when Fe II absorption lines were strong. It has been published in Kraemer et al. (2001). I retrieve it from the Multi-mission Archive at the Space Telescope Science Institute. The spectrum of SDSS J0839+3805 is taken from SDSS database. There exist no strong absorption lines at rest 1830 and 1840 \AA in the spectra of NGC 4151 and SDSS J0839+3805 (figure 5). Therefore, the trough between 1830 and 1840 \AA in the rest frame of $z = 2.0942$ must be Al III $\lambda\lambda 1854.7, 1862.8$ at $z = 2.053$.

The absorption at $\sim 5840 \text{ \AA}$ corresponds to Fe III UV34 $\lambda 1914.1$ at $z = 2.053$. However, the wavelength of Fe III UV34 $\lambda 1914.1$ at $z = 2.053$ is 5843.6 \AA , which is very close to the wavelength of Fe II UV125 $\lambda 1888.7$ at $z = 2.0942$, 5844.0 \AA . Fe II UV125 $\lambda\lambda 1877.5, 1888.7$, and 1894.0 is a triplet whose lower term (a^2H) are 2.51 – 2.57 eV above ground. The oscillator strength of Fe II UV125 is not available, however, the Fe II UV125 $\lambda 1877.5$ absorption line is stronger than or similar to the $\lambda 1888.7$ absorption line in the spectra of NGC 4151 and SDSS 0839+3805 (figure 5). On the other hand, in the spectrum of SDSS J1723+5553, the Fe II UV125 $\lambda 1877.5$ at $z = 2.0942$ absorption is too weak to identify (figure 5). Also, Fe II UV125 $\lambda 1888.7$ at $z = 2.0942$ must be weak, too. Other Fe II multiplets from excited terms (b^4P and a^4H) of 2.6 – 2.7 eV above ground, for example, Fe II UV148, 158, 159, and 161 between 2430 and 2560 \AA are weak in SDSS 1723+5553 (figure 6). In the other three Balmer BAL AGNs those absorption lines are strong and most of the continuum light is absorbed. Thus, the absorber of SDSS 1723+5553 has a lower density and/or lower temperature than the other three Balmer BAL AGNs. I can thus ignore the Fe II UV125 $\lambda 1888.7$ absorption at $z = 2.0942$. The absorption at $\sim 5840 \text{ \AA}$ must be Fe III UV34 $\lambda 1914.1$ absorption at $z = 2.053$.

The wavelength of Fe III UV34 $\lambda 1926.3$ at $z = 2.053$ is between Fe III UV34 $\lambda 1895.5$ at $z = 2.100$ and 2.1082 . I model Fe III UV34 $\lambda 1895.5 \text{ \AA}$ absorption at $z = 2.0942, 2.100$ and 2.1082 ,

¹ No spectrum between 1700 and 2000 \AA is currently available for SDSS J1259+1213.

and subtract it from the spectrum. First, I normalize the spectrum of SDSS 1723+5553 between 5800 and 6000 Å with a Legendre polynomial. The normalized spectrum of SDSS 1723+5553 is shown in the upper panel of figure 7. In order to make a model profile of Fe III UV34 $\lambda 1895.5$ Å absorption at $z = 2.0942, 2.100$ and 2.1082 , I fit profiles of Fe III UV34 $\lambda\lambda 1914.1, 1926.3$ at $z = 2.0942, 2.100$ and 2.1082 . I fix the ratio of intensity of the absorption as the ratio of each oscillator strength of the transition. The widths of the absorption troughs are same among components of the same redshift. The redshifts are fixed among the three transitions. I thus fit the normalized spectrum between 5900 Å and 6000 Å with a continuum and two absorption lines (Fe III UV34 $\lambda\lambda 1914.1, 1926.3$). I model Fe III UV34 $\lambda 1895.5$ based on the fitting results of Fe III $\lambda\lambda 1914.1, 1926.3$. The model profile of Fe III UV34 at $z = 2.0942, 2.100$ and 2.1082 is shown as the dashed line in the upper panel of figure 7. The fit is good for Fe III UV34 $\lambda\lambda 1914.1, 1926.3$. The result of the subtraction is shown in the lower panel of figure 7. The two absorption features remain at the wavelength of Fe III UV34 $\lambda\lambda 1914.1, 1926.3$ at $z = 2.053$. Fe III UV34 $\lambda 1895.5$ at $z = 2.053$ unfortunately overlaps with Al III emission and the absorption line (figure 4). It is difficult to deblend them. Hall et al. (2002) has pointed out unidentified absorption lines at 5840 and 5680 Å (observed frame) in SDSS J1723+5553 spectrum. Those unidentified absorption lines I identify as the $z = 2.053$ system of Fe III $\lambda 1914.1$ and Al III $\lambda\lambda 1854.7, 1862.8$, respectively.

I fit Fe III $\lambda 1914.1, 1926.3$ and Al III $\lambda\lambda 1854.7, 1862.8$ at $z = 2.053$ with gaussians in order to measure their widths. The Fe III absorption lines are fitted with two gaussians of the same width and redshift. The Al III absorption lines are also fitted with the same way. The FWHM_{true} of Fe III and Al III are 1030 ± 60 and 1350 ± 90 km s⁻¹, with redshifts of 2.0522 ± 0.0002 , 2.0517 ± 0.0004 , respectively. The FWHMs are consistent with those of the Balmer absorption lines.

5. Conclusion

I present the discovery of Balmer-series absorption lines from H α to H9 in SDSS J1723+5553 by near-infrared spectroscopy. The Balmer-line absorption is at $z = 2.053$ and blueshifted by 5370 km s⁻¹ from the Balmer emission lines. I derive the column density of neutral hydrogen of 5.2×10^{17} cm⁻² by the curve of growth method. The Balmer-line absorption is more than 4000 km s⁻¹ blueshifted from the previously known UV absorption lines. I search for the same velocity component seen in the UV absorption lines with Balmer-line absorption. I find the component at $z = 2.053$ in Al III and Fe III absorption lines.

High resolution near-infrared spectroscopy is needed to estimate a more precise column density of neutral hydrogen and covering factor of the absorber. If we can deblend He I $\lambda 3890$ from H8 absorption, we will be able to estimate ionized helium column density. He I $\lambda 3890$ absorption arises from the metastable $2\ ^3S$ level of He⁰. The population of the metastable $2\ ^3S$ is balanced by recombination to all triplet levels of He⁺ and collisional transition to other

levels. Also, search for other UV absorption at $z = 2.053$ by high resolution optical spectroscopy would be interesting. Farther if we can identify absorption troughs from the excited metastable level of Fe II and/or Si II, the derived relative populations will allow us to estimate the electron number density of the absorber associated with Balmer-line absorption. When combined with photoionization modeling, the distance of the absorber from the nucleus can be estimated. The Balmer absorption troughs translates to a large number of $n=2$ level hydrogen atoms, which is result of Ly α trapping. A high density and a high column density are necessary for Ly α trapping. This indicates that the outflow associated with Balmer absorption lines probably traces gas closer to nuclei. Combination of such high velocity of 5370 km s^{-1} and high column density, the mass flux of flow in SDSS 1723+5553 is probably as large as already measured in other FeLoBALs (Dunn et al. 2010).

I am grateful to the staffs of Subaru Telescope for their assistance during our observations. I also thank Toshihiro Kawaguchi and the anonymous referee for his or her helpful comments. I would also like to thank Jay P. Dunn for patient English proof reading. Funding for the Sloan Digital Sky Survey (SDSS) and SDSS-II has been provided by the Alfred P. Sloan Foundation, the Participating Institutions, the National Science Foundation, the U.S. Department of Energy, the National Aeronautics and Space Administration, the Japanese Monbukagakusho, and the Max Planck Society, and the Higher Education Funding Council for England. The SDSS Web site is <http://www.sdss.org/>. The SDSS is managed by the Astrophysical Research Consortium (ARC) for the Participating Institutions. The Participating Institutions are the American Museum of Natural History, Astrophysical Institute Potsdam, University of Basel, University of Cambridge, Case Western Reserve University, The University of Chicago, Drexel University, Fermilab, the Institute for Advanced Study, the Japan Participation Group, The Johns Hopkins University, the Joint Institute for Nuclear Astrophysics, the Kavli Institute for Particle Astrophysics and Cosmology, the Korean Scientist Group, the Chinese Academy of Sciences (LAMOST), Los Alamos National Laboratory, the Max-Planck-Institute for Astronomy (MPIA), the Max-Planck-Institute for Astrophysics (MPA), New Mexico State University, Ohio State University, University of Pittsburgh, University of Portsmouth, Princeton University, the United States Naval Observatory, and the University of Washington. This publication makes use of data products from the Two Micron All Sky Survey, which is a joint project of the University of Massachusetts and the Infrared Processing and Analysis Center/California Institute of Technology, funded by the National Aeronautics and Space Administration and the National Science Foundation. This research has also made use of the Atomic Line List, version 2.04, available at <http://www.pa.uky.edu/~peter/atomic/>.

References

Aoki, K., Iwata, I., Ohta, K., Ando, M., Akiyama, M., & Tamura, N. 2006, *ApJ*, 651, 84

Arav, N., Moe, M., Costantini, E., Korista, K., T., Benn, C., & Ellison, S. 2008, *ApJ*, 681, 954

Cecil, G., Dopita, M. A., Groves, B., Wilson, A. S., Ferruit, P., Pécontal, E., & Binette, L. 2002, *ApJ*, 568, 627

Crenshaw, D. M., Kraemer, S. B., Boggess, A., Maran, S. P., Moshotzky, R., F., & Wu, C.-C. 1999, *ApJ*, 516, 750

Crenshaw, D. M., & Kraemer, S. B. 2005, *ApJ*, 625, 680

Dunn, J. P., Crenshaw, D. M., Kraemer, S. B., Gabel, J. R. 2007, *AJ*, 134, 1061

Dunn, J. P., et al. 2010, *ApJ*, 709, 611

Fabian, A. C. 1999, *MNRAS*, 308, L39

Ganguly, R., & Brotherton, M. S. 2008, *ApJ*, 672, 102

Granato, G. L., De Zotti, G., Silva, L., Bressan, A., & Danese, L. 2004, *ApJ*, 600, 580

Greene, J. E. & Ho, L. C. 2005, *ApJ*, 630, 122

Hall, P. B., et al. 2002, *ApJS*, 141, 267

Hall, P. B. 2007, *AJ*, 133, 1271

Iye, M., et al. 2004, *PASJ*, 56, 381

Kraemer, S. B. et al. 2001, *ApJ*, 551, 671

Lynds, C. R. 1967, *ApJ*, 147, 396

Misawa, T., Charlton, J. C., Erachleous, M., Ganguly, R., Tytler, D., Kirkman, D., Suzuki, N., & Lubin, D. 2007, *ApJS*, 171, 1

Motohara, K., et al. 2002, *PASJ*, 54, 315

Netzer, H., Shemmer, O., Maiolino, R., Oliva, E., Croom, S., Corbett, E., & di Fabrizio, L. 2004, *ApJ*, 614, 558

Osterbrock, D. E., & Ferland, G. J. 2006, *Astrophysics of Gaseous Nebulae and Active Galactic Nuclei* 2nd Edition (Sausalito: University Science Books), 364

Savaglio, S., Fall, . M., & Fiore, F. 2003, *ApJ*, 585, 638

Silk, J. & Rees, M. J. 1998, *A&A*, 331, L1

Spitzer, L. 1978, in *Physical Processes in the Interstellar Medium* (New York: Wiley)

Turner, T. J., & Miller, L. 2009, *A&A Rev.*, 17, 47

York, D. G., et al. 2000, *AJ*, 120, 1579

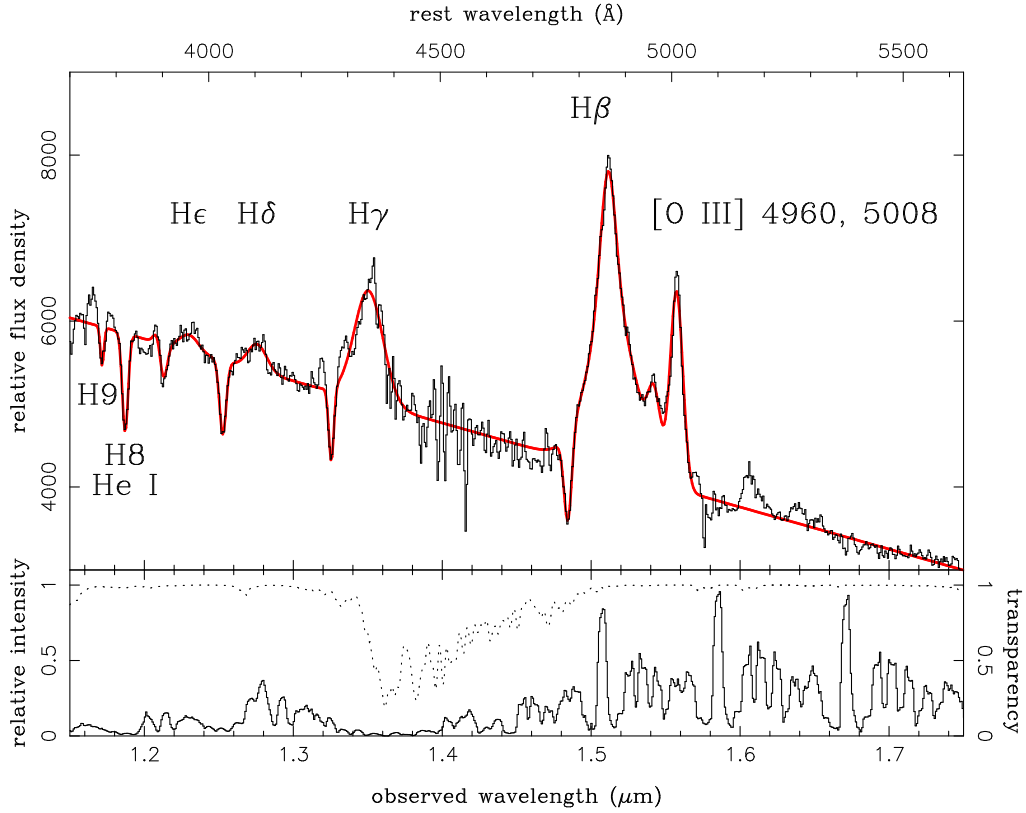


Fig. 1. Top: *JH*-band spectrum of SDSS J1723+5553. Ordinate is a relative flux density in units of $\text{erg s}^{-1} \text{cm}^{-2} \mu\text{m}^{-1}$, and abscissa is the observed wavelength in vacuum in microns. The rest wavelength is given along the top axis. The best fit result is shown as a red line. Bottom: The sky emission spectrum (solid line) and the atmospheric transmission curve (dotted line), which is obtained from the United Kingdom Infra-Red Telescope (UKIRT) Web page. It is produced using the program IRTRANS4.

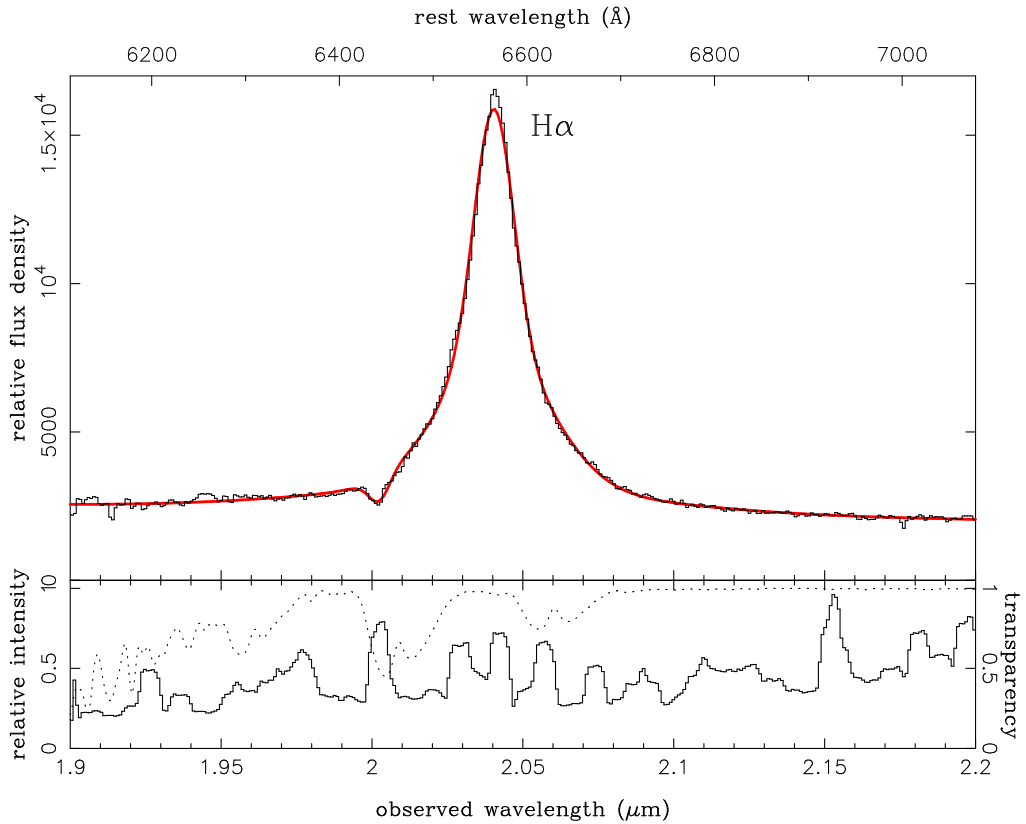


Fig. 2. Top: K -band spectrum of SDSS J1723+5553. Ordinate is a relative flux density in units of $erg s^{-1} cm^{-2} \mu m^{-1}$, and abscissa is the observed wavelength in vacuum in microns. The rest wavelength is given along the top axis. The H α emission line is fitted with three Gaussians. The best fit is shown as a red solid line. Bottom panel is as in Fig. 1.

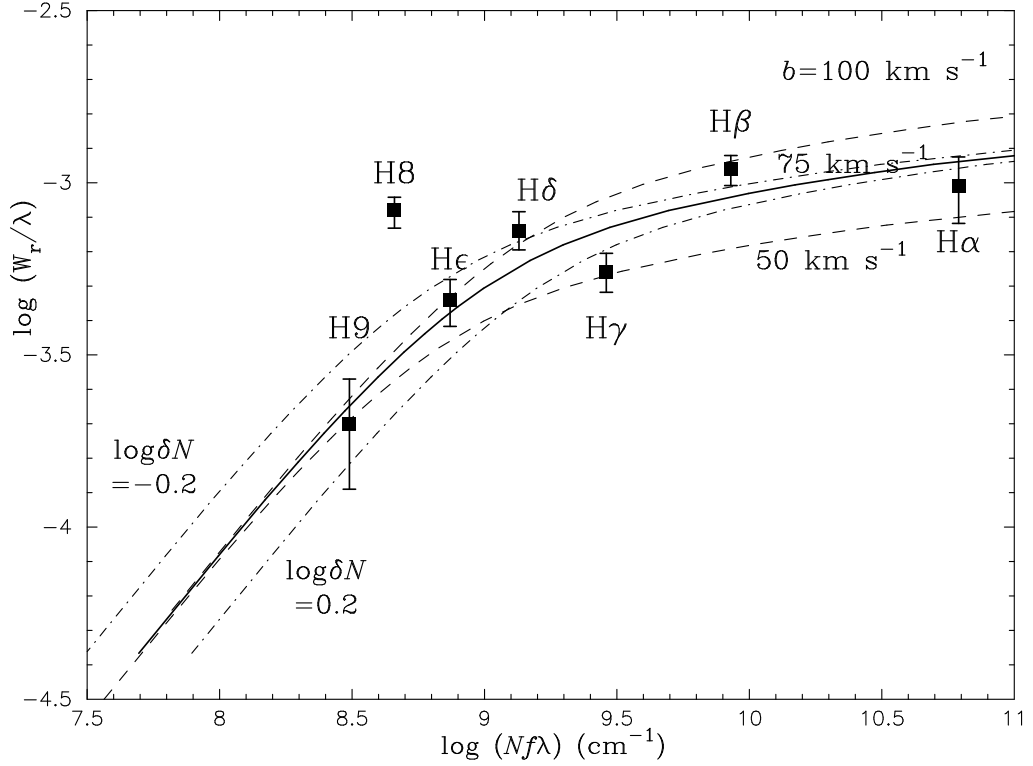


Fig. 3. The growth curve of Balmer-lines absorption. The best-fit curve of growth curve (75 km s^{-1} of b and $1.5 \times 10^{15} \text{ cm}^{-2}$ of the column density) is indicated by the solid line. The dashed-lines indicate the cases of 25 km s^{-1} larger and smaller than the best Doppler parameter. The do-dashed lines indicate the cases of 0.2 larger and smaller than the best column density in logarithmic scale. The strength of H8 clearly deviates from the curve of growth. This supports possible contamination of He I. I did not use H8 for the fitting.

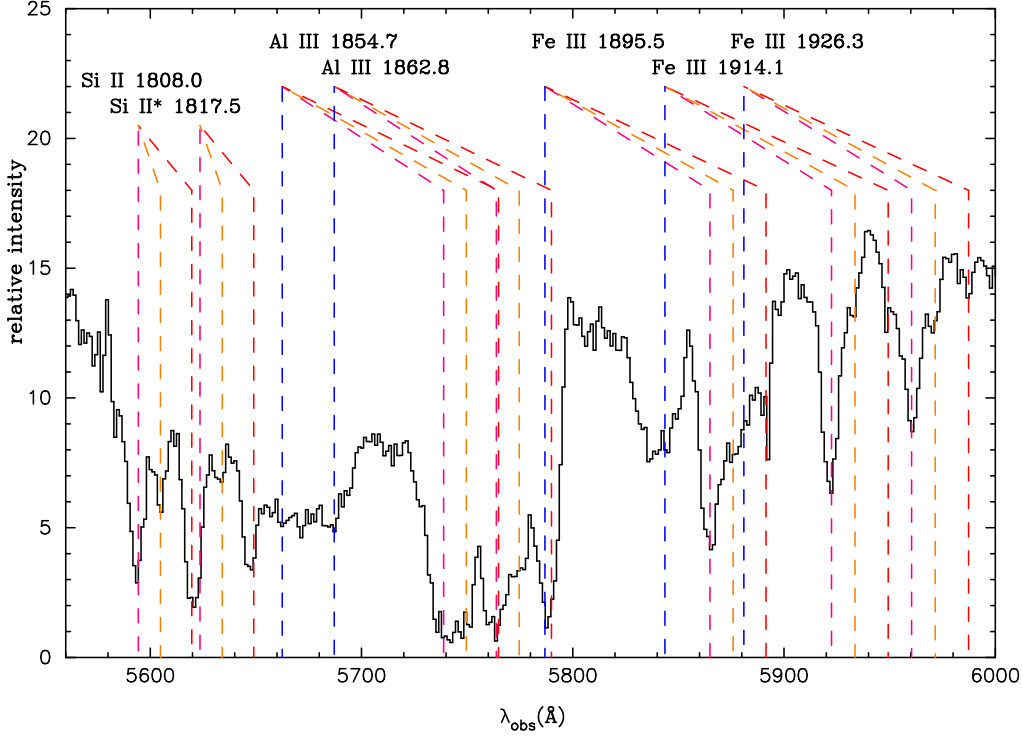


Fig. 4. Search for $z = 2.053$ system. The spectrum of SDSS J1723+5553 between 5540 Å and 6000 Å in observed frame is shown. The known absorption systems at $z = 2.0942, 2.100$ and 2.1082 are indicated by magenta, orange and red dashed lines, respectively. The expected positions of Al III and Fe III absorption lines at $z = 2.053$ are indicated by blue dashed lines.

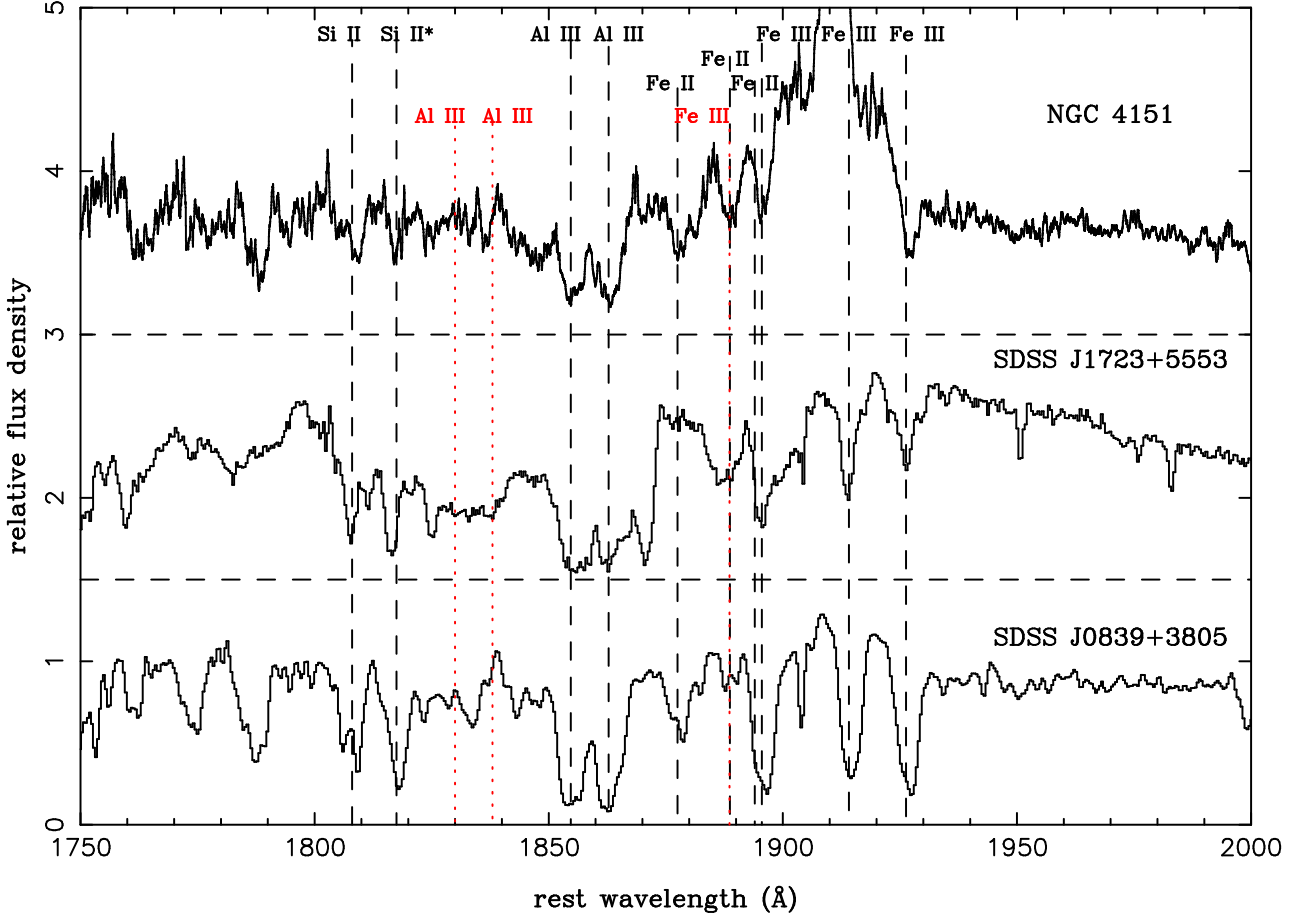


Fig. 5. Comparison of the spectrum of BAL AGN between 1700 and 2000 Å. Every spectrum is shifted to the frame of redshift of Al III absorption lines, and normalized by its continuum level. The redshift of 2.0942 is adopted for SDSS 1723+5553. Ordinate is a relative flux density in units of $\text{erg s}^{-1} \text{cm}^{-2} \text{\AA}^{-1}$. The spectra of SDSS 1723+5553 and NGC 4151 are offset by +1.5 and +3.0, respectively, for clarity, and their zero levels are shown by horizontal dashed lines. The vertical dashed lines indicate the positions of Si II 1808.0, Si II* 1817.5, Al III 1854.7, Al III 1862.8, Fe II UV125 1877.5, Fe II UV125 1888.7, Fe II UV125 1894.0, Fe III 1895.5, Fe III 1914.1, and Fe III 1926.3. The $z = 2.053$ system of Al III 1854.7, Al III 1862.8, and Fe III 1914.1 are indicated by vertical red dotted lines. The $z = 2.053$ system of Fe III 1914.1 coincides with Fe II UV125 1888.7 at $z = 2.0942$.

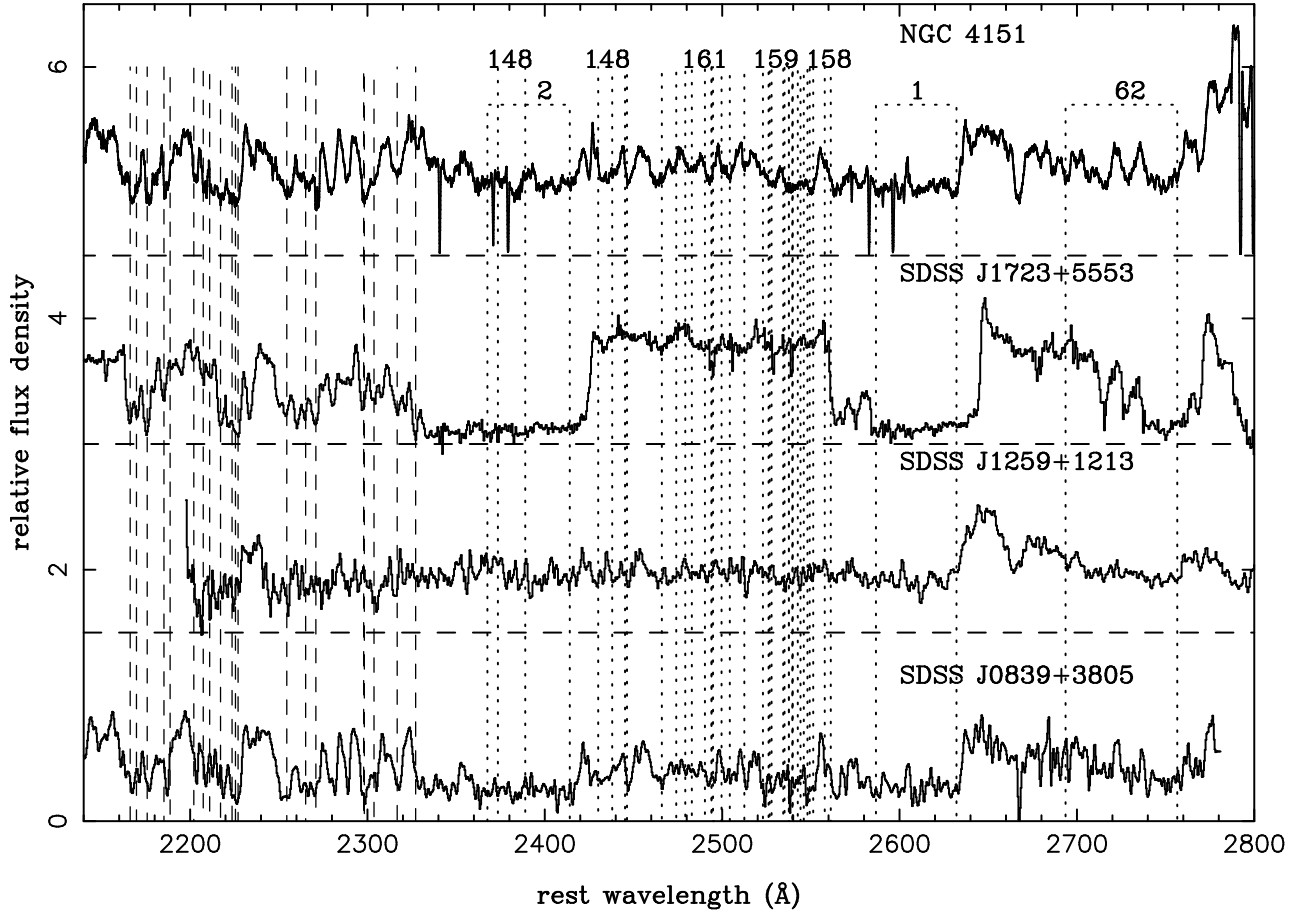


Fig. 6. Comparison of rest near UV spectra of Balmer BAL AGN. Every spectrum is shifted to the frame of redshift of Al III absorption lines, and normalized by its continuum level. Ordinate is a relative flux density in units of $\text{erg s}^{-1} \text{cm}^{-2} \text{\AA}^{-1}$. The spectra of SDSS 1259+1213, SDSS 1723+5553 and NGC 4151 are offset by +1.5, +3.0, and +4.5, respectively, for clarity, and their zero levels are shown by horizontal dashed lines. The vertical dashed lines between 2180 Å and 2340 Å indicate Ni II absorption lines. The dotted vertical lines indicate Fe II absorption lines, and the numbers indicate multiplets

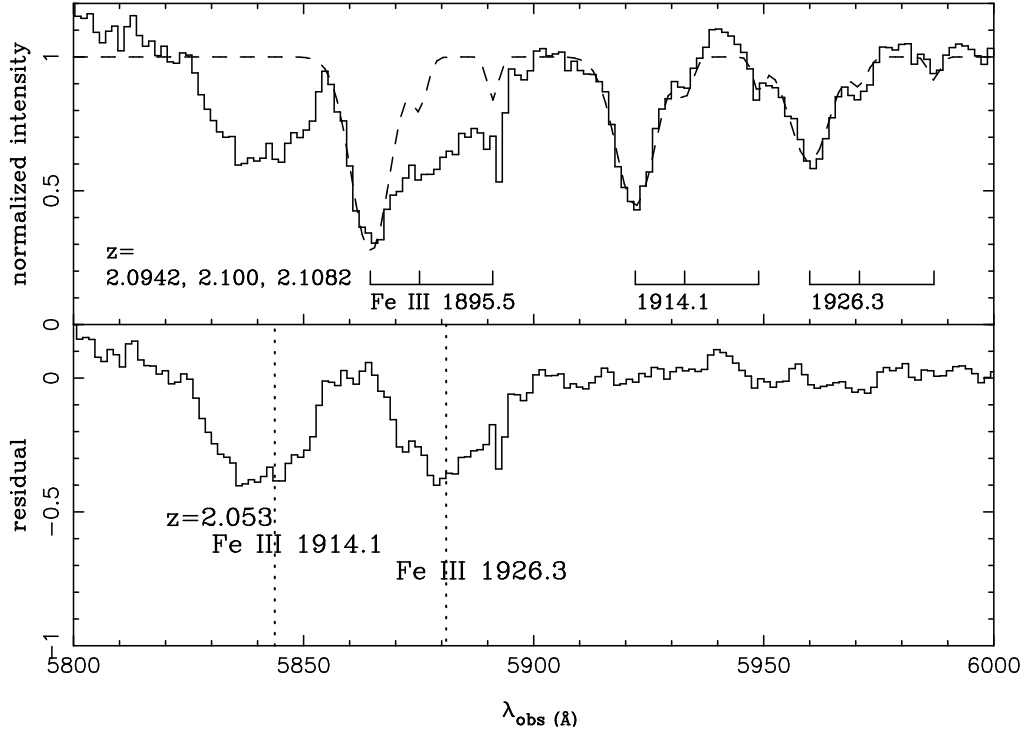


Fig. 7. Fe III absorption at $z = 2.053$. Top: The normalized spectrum of SDSS J1723+5553 between 5800 \AA and 6000 \AA in observed frame is shown in the histogram. The best fit of Fe III absorption at $z = 2.0942, 2.100$ and 2.1082 is shown in the dashed line. Note that the region between 5800 \AA and 5900 \AA was not used for the fitting. Bottom: The residual spectrum after subtraction of Fe III absorption at $z = 2.0942, 2.100$ and 2.1082 is shown in the histogram. The expected positions of Fe III $\lambda\lambda 1914.1, 1926.3$ absorption lines at $z = 2.053$ are indicated by the dotted lines. They clearly correspond to two absorption lines at $z = 2.053$.

Table 1. Properties of Emission and Absorption Lines.

Line	Absorption/Emission	z	FWHM _{true} (km s ⁻¹)
H α	Emission	2.1081 ± 0.0003	2780 ± 130
H β	Emission	2.1080 ± 0.0008	3780 ± 150
H γ^*	Emission	2.1107 ± 0.0012	–
H δ	Emission	2.1095 ± 0.0041	–
H ϵ	Emission	2.0973 ± 0.0057	–
[O III] 5008	Emission	2.1095 ± 0.0004	1550 ± 70
H α^{\dagger}	Absorption	2.0500 ± 0.0007	760 ± 300
H β	Absorption	2.0527 ± 0.0005	450 ± 130
H γ	Absorption	2.0530 ± 0.0006	< 890
H δ	Absorption	2.0532 ± 0.0008	520 ± 200
H ϵ	Absorption	2.0533 ± 0.0013	1000 ± 430
H8 ‡	Absorption	2.0517 ± 0.0006	< 710
H9	Absorption	2.0540 ± 0.0015	< 710

* H γ emission is affected by the atmospheric absorption lines.

† H α absorption is affected by the atmospheric absorption lines.

‡ H8 absorption is probably blended with He I 3890 absorption line.

Table 2. Equivalent widths of Balmer absorption lines.

	λ Å	f oscillator strength	EW_{rest} Å
H α	6564.610	6.40E-01	$6.4 \pm 1.4^*$
H β	4862.683	1.19E-01	5.3 ± 0.53
H γ	4341.684	4.46E-02	2.4 ± 0.31
H δ	4102.892	2.21E-02	3.0 ± 0.38
H ϵ	3971.195	1.27E-02	1.8 ± 0.28
H8	3890.151	8.03E-03	$3.2 \pm 0.33^{\dagger}$
H9	3836.472	5.43E-03	0.76 ± 0.27

* H α absorption is affected by the atmospheric absorption lines.

\dagger H8 absorption is probably blended with He I 3890 absorption line.